d-wave superconductivity in boson+fermion dimer models

Garry Goldstein, Claudio Chamon, and Claudio Castelnovo

Phys. Rev. B **95**, 174511 — Published 18 May 2017

DOI: 10.1103/PhysRevB.95.174511

d-wave superconductivity in boson+fermion dimer models

Garry Goldstein,[1] Claudio Chamon,[2] and Claudio Castelnovo[1]

[1] *TCM Group, Cavendish Laboratory, University of Cambridge, J. J. Thomson Avenue, Cambridge CB3 0HE, United Kingdom*

[2] *Department of Physics, Boston University, Boston, Massachusetts 02215, USA*

We present a slave-particle mean-field study of the mixed boson+fermion quantum dimer model introduced by Punk, Allais, and Sachdev [PNAS **112**, 9552 (2015)] to describe the physics of the pseudogap phase in cuprate superconductors. Our analysis naturally leads to four charge e fermion pockets whose total area is equal to the hole doping p, for a range of parameters consistent with the $t-J$ model for high temperature superconductivity. Here we find that the dimers are unstable to d-wave superconductivity at low temperatures. The region of the phase diagram with d-wave rather than s-wave superconductivity matches well with the appearance of the four fermion pockets. In the superconducting regime, the dispersion contains eight Dirac cones along the diagonals of the Brillouin zone.

PACS numbers:

I. INTRODUCTION

The Rokhsar-Kivelson quantum dimer model (QDM) was originally introduced to describe a possible magnetically-disordered phase – the resonating valence bond (RVB) phase – in high-temperature superconducting materials [1]. The arena where the QDM has been deployed has greatly expanded since its inception, and the model has taken on a key role in the study of a variety of magnetic quantum systems. Quantum dimers show up prominently in the study of hard-core bosons hopping on frustrated lattices [2], of arrays of Josephson junctions with capacitative and Josephson couplings [3], of frustrated Ising models with an external field or with perturbative XY couplings [4], of various types of gauge theories [5], and of models with large spin-orbit couplings [6] and various cold atom setups [7]. The study of QDMs led to an abundance of new phenomena including deconfined quantum criticality and new routes to deconfinement [8]. It also provided one of the earliest known examples of topologically ordered states in a lattice model [9].

Recently QDMs have been revisited as models of high-temperature superconductivity [10–12]. This was motivated by the need to reconcile transport experiments [13–16] and photoemission data [17–19] in the underdoped region of cuprate superconductors: while photoemission data show Fermi arcs enclosing an area $1+p$ (with p being the doping), transport measurements indicate plain Fermi-liquid properties consistent with an area p. In order to resolve this issue and produce a Fermi liquid which encloses an area p, the authors of Refs. [10–12] introduced a model for the pseudogap region of the cuprate superconductors which consists of two types of dimers: one spinless bosonic dimer – representing a valence bond between two neighboring spins – and one spin 1/2 fermionic dimer representing a hole delocalized between two sites. Fig. 1 shows an example of a boson+fermion dimer covering of the square lattice and depicts the dimer moves dictated by the quantum Hamiltonian in Eq. (2). The boson+fermion QDM (bfQDM) was introduced and studied numerically in Ref. 10 using exact diagonalization, supporting the existence of a fractionalized Fermi liquid enclosing an area p.

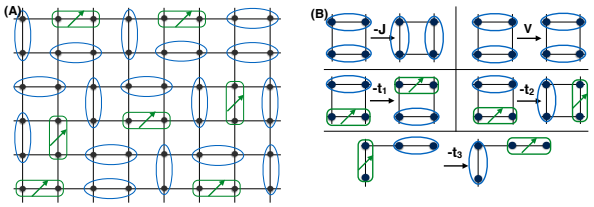

Figure 1: The boson+fermion quantum dimer model of Ref. 10. (A) A particular dimer configuration. The lattice is shown in black. The bosonic dimers representing the valence bonds are shown in blue while the spinful fermionic dimers representing a single electron delocalized over two sites are shown in green. (B) Diagrams representative of the various terms in the dimer Hamiltonian Eq. (2).

In this work we present a slave boson and fermion formulation of the bfQDM. We find that four symmetric fermion pockets, located in the vicinity of $\left(\pm\frac{\pi}{2},\pm\frac{\pi}{2}\right)$ in the Brillouin zone, naturally appear at mean-field level. The total area of the four pockets is given by the hole (fermionic) doping. We find that the system is unstable to d-wave superconductivity at low temperatures. The region of the phase diagram with d-wave superconductivity matches well the region with four fermion pockets. In the superconducting phase, the fermionic dimers (holes) acquire a Dirac dispersion at eight points along the diagonals of the Brillouin zone.

II. MAPPING ONTO SLAVE BOSON/FERMION MODEL

The quantum dimer model can be mapped exactly onto a slave boson+fermion model by considering a secondary Hilbert space where we assign to each link $(i, i+\eta)$ of the lattice ($\eta = \hat{x}, \hat{y}$) a bosonic mode $b_{i,\eta}$ and a spinful fermionic mode $c_{i,\eta,\sigma}$ ($\sigma =\uparrow,\downarrow$). We associate the number of dimers on a link with the occupation numbers of the bosons or fermions on that link. As such we have embedded the dimer Hilbert space in a larger boson/fermion Hilbert space. The constraint that each site of the lattice has one and exactly one dimer attached to it may be rephrased in the boson/fermion language as:

$$\Pi_i \equiv \sum_{l\in v_i} b_l^\dagger b_l + c_{l,\uparrow}^\dagger c_{l,\uparrow} + c_{l,\downarrow}^\dagger c_{l,\downarrow} - 1 = 0\,. \qquad (1)$$

Here, for convenience of notation, $\ell \in v_i$ labels the four links j, η that are attached to vertex i. Any Hamiltonian for the dimers has a boson/fermion representation; in particular the terms illustrated in Fig. 1B can be written as:

$$\begin{aligned} H_D = &\sum_i \Big\{ -J\, b_{i,\hat{x}}^\dagger b_{i+\hat{y},\hat{x}}^\dagger b_{i,\hat{y}} b_{i+\hat{x},\hat{y}} + 1 \text{ term} \\ &+V\, b_{i,\hat{x}}^\dagger b_{i,\hat{x}} b_{i+\hat{y},\hat{x}}^\dagger b_{i+\hat{y},\hat{x}} + 1 \text{ term} \Big\} \\ &\sum_i \sum_\sigma \Big\{ -t_1\, b_{i,\hat{x}}^\dagger c_{i+\hat{y},\hat{x},\sigma}^\dagger c_{i,\hat{x},\sigma} b_{i+\hat{y},\hat{x}} + 3 \text{ terms} \\ &- t_2\, b_{i+\hat{x},\hat{y}}^\dagger c_{i,\hat{y},\sigma}^\dagger c_{i,\hat{x},\sigma} b_{i+\hat{y},\hat{x}} + 7 \text{ terms} \\ &- t_3\, b_{i+\hat{x}+\hat{y},\hat{x}}^\dagger c_{i,\hat{y},\sigma}^\dagger c_{i+\hat{x}+\hat{y},\hat{x},\sigma} b_{i,\hat{y}} + 7 \text{ terms} \\ &-t_3\, b_{i+2\hat{y},\hat{x}}^\dagger c_{i,\hat{y},\sigma}^\dagger c_{i+2\hat{y},\hat{x},\sigma} b_{i,\hat{y}} + 7 \text{ terms} \Big\} \\ &- \mu \sum_i \sum_\sigma \sum_\eta c_{i,\eta,\sigma}^\dagger c_{i,\eta,\sigma}\,, \end{aligned} \qquad (2)$$

where we included a chemical potential for the holes (fermionic dimers), which is important for the connection with doped high-temperature superconductors [20, 21]. The terms not written explicitly in Eq. (2) are simply obtained from those shown by translational symmetry, four fold rotational symmetry, and reflection symmetry about the two diagonals. This Hamiltonian also has a local $U(1)$ gauge symmetry

$$b_{i,\eta} \to e^{i\theta_i}\, b_{i,\eta}\, e^{i\theta_{i+\eta}}\,, \quad c_{i,\eta,\sigma} \to e^{i\theta_i}\, c_{i,\eta,\sigma}\, e^{i\theta_{i+\eta}}\,, \quad (3)$$

with a phase θ_i associate to each vertex i. Any Hamiltonian that preserves the constraint given in Eq. (1) is invariant under this gauge transformation [22, 23].

A slave boson/fermion formulation of the bfQDM is obtained by introducing a Lagrange multiplier: a real field $\lambda_i(\tau)$ that enforces the dimer constraint Eq. (1) at all times τ, and shifting the action by $\Delta\mathcal{S} = -\int d\tau \sum_i \lambda_i(\tau)\,\Pi_i(\tau)$.

III. SLAVE BOSON/FERMION MEAN-FIELD DECOUPLING

A systematic mean-field approach can be obtained by taking the saddle point with respect to the Lagrange multiplier field $\lambda_i(\tau) \to \lambda_i$, with a time-independent value λ_i that enforces the average constraint $\langle\Pi_i\rangle = 0$. This procedure is accompanied by Hubbard Stratonovich (HS) transformations of every term in the Hamiltonian in Eq. (2) separately. We begin with the purely bosonic potential term:

$$\begin{aligned} &b_{i,\hat{x}}^\dagger b_{i,\hat{x}} b_{i+\hat{y},\hat{x}}^\dagger b_{i+\hat{y},\hat{x}} \to \\ &\kappa_1 \left\{ b_{i,\hat{x}}^\dagger b_{i,\hat{x}}\, x_{i1} + b_{i+\hat{y},\hat{x}}^\dagger b_{i+\hat{y},\hat{x}}\, x_{i2} - x_{i1} x_{i2} \right\} \\ &+ (1-\kappa_1) \left\{ b_{i,\hat{x}}^\dagger b_{i+\hat{y},\hat{x}}^\dagger\, z_i + b_{i,\hat{x}} b_{i+\hat{y},\hat{x}}\, z_i^* - \left|z_i^2\right| \right\}, \end{aligned} \qquad (4)$$

where x_i and z_i are auxiliary fields to be integrated over and κ_1 is arbitrary. At mean-field level we can drop the integrals over the auxiliary fields and replace them with their saddle point values $x_{i1} \to \langle b_{i+\hat{y},\hat{x}}^\dagger b_{i+\hat{y},\hat{x}}\rangle$, $x_{i2} \to \langle b_{i,\hat{x}}^\dagger b_{i,\hat{x}}\rangle$ and $z_i \to \langle b_{i,\hat{x}} b_{i+\hat{y},\hat{x}}\rangle$. The hopping term may be decoupled in a similar manner:

$$\begin{aligned} &b_{i,\hat{x}}^\dagger b_{i+\hat{y},\hat{x}}^\dagger b_{i,\hat{y}} b_{i+\hat{x},\hat{y}} + \text{h.c.} \to \\ &\kappa_2 \left\{ b_{i,\hat{x}}^\dagger b_{i+\hat{y},\hat{x}}^\dagger\, w_{i1} + b_{i,\hat{y}} b_{i+\hat{x},\hat{y}}\, w_{i2}^* - w_{i1} w_{i2}^* + \text{h.c.} \right\} \\ &+ (1-\kappa_2) \left\{ b_{i,\hat{x}}^\dagger b_{i,\hat{y}}\, q_{i1} + b_{i+\hat{y},\hat{x}}^\dagger b_{i+\hat{x},\hat{y}}\, q_{i2}^* - q_{i1} q_{i2}^* + \text{h.c.} \right\}, \end{aligned} \qquad (5)$$

where, again, at mean-field level we use the saddle point values $w_{i1} \to \langle b_{i,\hat{y}} b_{i+\hat{x},\hat{y}}\rangle$, $w_{i2}^* \to \langle b_{i,\hat{x}}^\dagger b_{i+\hat{y},\hat{x}}^\dagger\rangle$, $q_{i1} \to \langle b_{i+\hat{y},\hat{x}}^\dagger b_{i+\hat{x}\,,\hat{y}}\rangle$, $q_{i2}^* \to \langle b_{i,\hat{x}}^\dagger b_{i,\hat{y}}\rangle$ and κ_2 is arbitrary. Other HS decouplings, and linear combinations thereof, are also possible.

We can make substantial progress in understanding the fermionic component of the theory without detailed analysis of the bosonic component. Indeed, any translationally invariant (liquid-like) bosonic ansatz yields similar fermionic effective theories. The fermionic mean-field Hamiltonian reads

$$\begin{aligned} H_{F\bar{B}} = &\sum_\sigma \sum_i \Big\{ -t_1\, c_{i+\hat{y},\hat{x},\sigma}^\dagger c_{i,\hat{x},\sigma} \langle b_{i,\hat{x}}^\dagger b_{i+\hat{y},\hat{x}}\rangle + 3 \text{ terms} \\ &- t_2\, c_{i,\hat{y},\sigma}^\dagger c_{i,\hat{x},\sigma} \langle b_{i+\hat{x},\hat{y}}^\dagger b_{i+\hat{y},\hat{x}}\rangle + 7 \text{ terms} \\ &- t_3\, c_{i,\hat{y},\sigma}^\dagger c_{i+\hat{x}+\hat{y},\hat{x},\sigma} \langle b_{i+\hat{x}+\hat{y},\hat{x}}^\dagger b_{i,\hat{y}}\rangle + 7 \text{ terms} \\ &-t_3\, c_{i,\hat{y},\sigma}^\dagger c_{i+2\hat{y},\hat{x},\sigma} \langle b_{i+2\hat{y},\hat{x}}^\dagger b_{i,\hat{y}}\rangle + 7 \text{ terms} \Big\} + \\ &(-2\lambda - \mu) \sum_i \sum_\sigma \sum_\eta c_{i,\eta,\sigma}^\dagger c_{i,\eta,\sigma}\,, \end{aligned} \qquad (6)$$

which is effectively a tight-biding model with renormalized hoppings $T_1 = t_1\, \langle b_{i,\hat{x}}^\dagger b_{i+\hat{y},\hat{x}}\rangle$, $T_2 = t_2\, \langle b_{i+\hat{x},\hat{y}}^\dagger b_{i+\hat{y},\hat{x}}\rangle$ and $T_3 = t_3\, \langle b_{i+\hat{x}+\hat{y},\hat{x}}^\dagger b_{i,\hat{y}}\rangle$.

The resulting model is defined on the bipartite checkerboard lattice that is medial to the original square lattice. The horizontal (x) and vertical (y) links make up the two sublattices where the fermions reside. We define (in momentum space) the spinor that encodes these two flavors as $\psi^\dagger_{\vec{k},\sigma} = (c^\dagger_{\vec{k},\hat{y},\sigma}, c^\dagger_{\vec{k},\hat{x},\sigma})$ and

$$H_{F\bar{B}} = \sum_{\vec{k},\sigma} \psi^\dagger_{\vec{k},\sigma} \begin{pmatrix} \xi^x_{\vec{k}} & \gamma_{\vec{k}} \\ \gamma^*_{\vec{k}} & \xi^y_{\vec{k}} \end{pmatrix} \psi_{\vec{k},\sigma} \ , \tag{7}$$

where:

$$\begin{aligned} \xi^x_{\vec{k}} &= -2\lambda - \mu - 2\,T_1\ \cos k_x \\ \xi^y_{\vec{k}} &= -2\lambda - \mu - 2\,T_1\ \cos k_y \\ \gamma_{\vec{k}} &= 4e^{i(k_y-k_x)/2}\ \left(T_2\ \cos\frac{k_x}{2}\cos\frac{k_y}{2} \right. \\ &\quad \left. + T_3\ \cos\frac{3k_x}{2}\cos\frac{k_y}{2} + T_3\ \cos\frac{k_x}{2}\cos\frac{3k_y}{2} \right). \end{aligned}$$

The eigenvalues are given by $E_{\pm,\vec{k}} = \xi_{\vec{k}} \pm \sqrt{\eta^2_{\vec{k}} + |\gamma_{\vec{k}}|^2}$, where $\xi_{\vec{k}} = (\xi^x_{\vec{k}} + \xi^y_{\vec{k}})/2$ and $\eta_{\vec{k}} = (\xi^x_{\vec{k}} - \xi^y_{\vec{k}})/2$. For hole doping p (the number of fermions in our model) the lower band $E_{-,\vec{k}}$ will be partially occupied. The total area enclosed by the Fermi surface in the lower band is equal to the hole doping p (multiplied by $4\pi^2$).

The Hamiltonian Eq. (7) has four-fold rotational symmetry, $k_x \to k_y$ and $k_y \to -k_x$, and reflection symmetry about the diagonals $k_x \to k_y$ and $k_y \to k_x$ as well as $k_x \to -k_y$ and $k_y \to -k_x$. Depending on the relative values of T_1, T_2 and T_3, the band minima will be located at different points in the Brillouin zone, and the Fermi surface topology will vary accordingly. In Fig. 2A we show the position of the minima along the $k_x = \pm k_y$ directions (or $\Gamma - M$ line), as a function of the ratios T_3/T_1 and T_2/T_1. We identify two regions in parameter space, where the dispersion minima are (i) at the Γ point (blue-colored region), and (ii) in between the Γ and M points, varying continuously with $T_1/T_3 - T_2/T_3$ (faded region). An example of dispersion where the minima are at $(k_x, k_y) \simeq (\pm\pi/2, \pm\pi/2)$ is shown in the bottom inset of Fig. 2A. Case (ii) is clearly conducive to the appearance of four Fermi pockets in an appropriate range of the chemical potential.

IV. D-WAVE SUPERCONDUCTIVITY

To study superconducting instabilities we need to include four-fermion terms in the Hamiltonian, i.e., go beyond the model introduced in Refs. 10–12 and summarized in Fig. 1B and Eq. (2). Consider the $t-J$ Hamiltonian on the square lattice [24],

$$H_{tJ} = -\sum_{\alpha} t_{ij} d^\dagger_{i,\alpha} d_{j,\alpha} + J \sum_{\langle i,j\rangle} \left(\vec{S}_i \cdot \vec{S}_j - \frac{1}{4} n_i n_j \right) \tag{8}$$

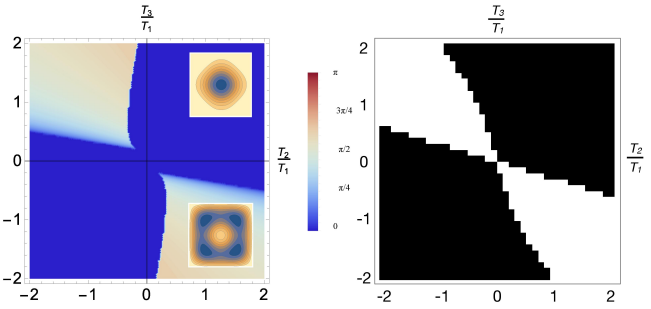

Figure 2: (A) Location of the band minima as a function of T_3/T_1 and T_2/T_1 (for $T_1 = 1$). The color scale corresponds to the distance along the $\Gamma - M$ line in the Brillouin zone: blue corresponds to the Γ point, $k_x = k_y = 0$, and red corresponds to the M point, $k_x = k_y = \pi$. The insets show contours of the dispersion of the lower band of the Hamiltonian Eq. (6) for specific choices of parameters in the corresponding regions. (B) Dominant superconductivity instability as a function of T_3/T_1 and T_2/T_1 for doping $p = 0.25$ and $J = 50$: d-wave (white) *vs.* s-wave (black). Note the good correlation between d-wave superconductivity and the appearance of four band minima.

subject to the constraint that $n_i \leq 1$. Here $d^\dagger_{i,\alpha}$ and $d_{i,\alpha}$ are the electron creation and annihilation operators ($\alpha = \uparrow, \downarrow$) of the $t-J$ model, $\vec{S}_i = d^\dagger_{i,\alpha}\, \vec{\sigma}_{\alpha,\beta}\, d_{i,\beta}$ (with α, β summed over), and $n_i = d^\dagger_{i,\uparrow} d_{i,\uparrow} + d^\dagger_{i,\downarrow} d_{i,\downarrow}$.

We can identify the dimer Hilbert space with a subspace of the Hilbert space for the $t-J$ model, where the zero dimers state corresponds to the state with zero electrons, and the rest of the Hilbert space can be introduced via the operators $b^\dagger_{i,\eta} \Leftrightarrow \Upsilon_{i,\eta}\, (d^\dagger_{i\uparrow} d^\dagger_{i+\eta\downarrow} - d^\dagger_{i\downarrow} d^\dagger_{i+\eta\uparrow})/\sqrt{2}$ and $c^\dagger_{i,\eta,\sigma} \Leftrightarrow \Upsilon_{i,\eta}(d^\dagger_{i,\sigma} + d^\dagger_{i+\eta,\sigma})/\sqrt{2}$. The phases $\Upsilon_{i,\eta}$ represent a gauge choice and we shall follow the one by Rokhsar and Kivelson [1] and define $\Upsilon_{i,\hat{y}} = 1$ and $\Upsilon_{i,\hat{x}} = (-1)^{i_y}$, where i_y is the y-component of the 2D square lattice site index i.

Given the conventional inner product for the electron Hilbert space, the dimer basis is not orthonormal. This issue can be addressed in general by Gram-Schmidt orthogonalization [25]; however, it is customary to use the leading order approximation and to assume that the dimer states are orthogonal (and normalized) [23]. The relevant Hamiltonian can then be determined by projecting Eq. (8) onto this basis. The pairing term (four-fermion interaction) comes from the spin-spin term in the $t-J$ model, namely $H_J = J \sum_{\langle i,j\rangle} \left(\vec{S}_i \cdot \vec{S}_j - \frac{1}{4} n_i n_j \right)$. Let us focus on a single plaquette term and consider eight relevant states for this plaquette, $c^\dagger_{i,\hat{x},\alpha} c^\dagger_{i+\hat{y},\hat{x},\beta} |0\rangle$ and $c^\dagger_{i,\hat{y},\alpha} c^\dagger_{i+\hat{x},\hat{y},\beta} |0\rangle$, $\alpha, \beta = \uparrow, \downarrow$. The Hamiltonian H_J is non-zero only in the singlet channel and therefore we must restrict the spins α, β to be in a singlet state, thereby the effective Hamiltonian for the dimers is given by $\tilde{H}_J = \begin{pmatrix} -J/2 & 0 \\ 0 & -J/2 \end{pmatrix}$ [23]. As such we add to our Hamil-

tonian in Eq. (2) the term:

$$\tilde{H}_J = -\frac{J}{4}\sum_i \left(\epsilon_{\alpha\gamma}\, c^\dagger_{i,\hat{x},\alpha}\, c^\dagger_{i+\hat{y},\hat{x},\gamma}\right)\left(\epsilon_{\beta\delta}\, c_{i+\hat{y},\hat{x},\beta}\, c_{i,\hat{x},\delta}\right) + x \leftrightarrow y\,. \tag{9}$$

For convenience we define $\Delta_x = \epsilon_{\alpha\gamma}\langle c^\dagger_{i,\hat{y},\alpha}\, c^\dagger_{i+\hat{x},\hat{y},\gamma}\rangle$ and $\Delta_y = \epsilon_{\alpha\gamma}\langle c^\dagger_{i,\hat{x},\alpha}\, c^\dagger_{i+\hat{y},\hat{x},\gamma}\rangle$, whereby d-wave pairing corresponds to $\Delta_x = -\Delta_y = \Delta$ (which in turn can be chosen real with an appropriate choice of phase). Using a HS transformation on Eq. (9), $H = \sum_{\vec{k}} \Psi^\dagger_{\vec{k}}\, \mathcal{H}_{\vec{k}}\, \Psi_{\vec{k}}$, where

$$\mathcal{H}_{\vec{k}} = \begin{pmatrix} \xi^x_{\vec{k}} & \gamma_{\vec{k}} & \Delta^x_{\vec{k}} & 0 \\ \gamma^*_{\vec{k}} & \xi^y_{\vec{k}} & 0 & \Delta^y_{\vec{k}} \\ \Delta^x_{\vec{k}} & 0 & -\xi^x_{-\vec{k}} & -\gamma_{-\vec{k}} \\ 0 & \Delta^y_{\vec{k}} & -\gamma^*_{-\vec{k}} & -\xi^y_{-\vec{k}} \end{pmatrix}, \tag{10}$$

and $\Psi^\dagger_{\vec{k}} = (c^\dagger_{\vec{k},\hat{y},\uparrow}, c^\dagger_{\vec{k},\hat{x},\uparrow}, c_{-\vec{k},\hat{y},\downarrow}, c_{-\vec{k},\hat{x},\downarrow})$. Here $\Delta^x_{\vec{k}} = \frac{J}{2}\Delta_x \cos k_x$ and $\Delta^y_{\vec{k}} = \frac{J}{2}\Delta_y \cos k_y$. The eigenvalues of this Hamiltonian are given by

$$E_{\pm,\pm,\vec{k}} = \pm\sqrt{\Theta_{\vec{k}} \pm \sqrt{\Lambda_{\vec{k}} + \Xi_{\vec{k}}}} \tag{11}$$

where

$$\Theta_{\vec{k}} = \frac{1}{2}\left[(\xi^x_{\vec{k}})^2 + (\xi^y_{\vec{k}})^2 + (\Delta^x_{\vec{k}})^2 + (\Delta^y_{\vec{k}})^2 + 2|\gamma_{\vec{k}}|^2\right]$$
$$\Lambda_{\vec{k}} = \frac{1}{4}\left[(\xi^x_{\vec{k}})^2 - (\xi^y_{\vec{k}})^2 + (\Delta^x_{\vec{k}})^2 - (\Delta^y_{\vec{k}})^2\right]^2$$
$$\Xi_{\vec{k}} = |\gamma_{\vec{k}}|^2\left[(\xi^x_{\vec{k}} + \xi^y_{\vec{k}})^2 + (\Delta^x_{\vec{k}} - \Delta^y_{\vec{k}})^2\right].$$

When T_1, T_2 and T_3 are such that there are four Fermi pockets (in the absence of superconductivity), there are eight Dirac points in the dispersion, i.e., there are eight nodes where the gap $E_{+,-,\vec{k}} = E_{-,-,\vec{k}} = 0$. These points are located along the diagonals of the Brillouin zone. When $k_x = \pm k_y$, $\Lambda_{\vec{k}}$ vanishes, and the gap closing condition $\Theta_{\vec{k}} = \sqrt{\Xi_{\vec{k}}}$ is equivalent to $\xi^2_{\vec{k}} + \Delta^2_{\vec{k}} - |\gamma_{\vec{k}}|^2 = 0$, where $\xi_{\vec{k}} = (\xi^x_{\vec{k}} + \xi^y_{\vec{k}})/2$ and $\Delta_{\vec{k}} = (\Delta^x_{\vec{k}} - \Delta^y_{\vec{k}})/2$. Notice that the Fermi surface in the absence of superconductivity is given by $\xi^2_{\vec{k}} - |\gamma_{\vec{k}}|^2 = 0$. Therefore, whenever there are four Fermi pockets, for a range of $\Delta^2_{\vec{k}}$ there will be two nodes for each pocket, slightly shifted along the diagonal from the original Fermi surface [23].

Using self consistent equations for the superconducting order parameter, we can then compare s-wave and d-wave instabilities. Up to an unimportant constant energy shift, the Gibbs free energy is given by

$$G = \frac{J}{4}\left(|\Delta^2_x| + |\Delta^2_y|\right) - \frac{2}{\beta}\int \frac{d^2k}{4\pi^2} \ln\left[\cosh\left(\frac{\beta}{2}E_{+,+,\vec{k}}\right)\cosh\left(\frac{\beta}{2}E_{+,-,\vec{k}}\right)\right]. \tag{12}$$

Minimizing the free energy with respect to Δ_x, we obtain:

$$\Delta_x = \sum_{s=\pm}\int \frac{d^2k}{4\pi^2}\, \frac{\tanh\left(\frac{\beta}{2}E_{+,s,\vec{k}}\right)\cos(k_x)}{2E_{+,s,\vec{k}}} \times \left\{\Delta^x_{\vec{k}} + \frac{s}{\sqrt{\Lambda_{\vec{k}} + \Xi_{\vec{k}}}}\left[\sqrt{\Lambda_{\vec{k}}}\,\Delta^x_{\vec{k}} + |\gamma_{\vec{k}}|^2\left(\Delta^x_{\vec{k}} - \Delta^y_{\vec{k}}\right)\right]\right\} \tag{13}$$

and similarly for Δ_y. From the symmetries of this equation we see that there are two solutions, $\Delta_x = \mp\Delta_y$, corresponding to d-wave and extended s-wave superconductivity.

We numerically compare the two solutions at zero temperature and find that d-wave superconductivity wins for a large range of ratios T_2/T_1 and T_3/T_1, as illustrated in Fig. 2B. The correlation between the region with fermion pockets depicted in Fig 2A and the region with d-wave superconductivity in Fig. 2B is evident [23]. This can be qualitatively understood as the largest change in the Gibbs free energy upon entering the superconducting state comes from the contribution of the integral around the FS. Since the shape of the four Fermi pockets follows largely the nodal lines of the s-wave order parameter, and it anti-correlates with the d-wave nodal lines, one expects the appearance of the pockets to favor d-wave superconductivity.

Whereas the horizontal boundaries match very well in the two panels in Fig. 2, the vertical boundaries less so. Indeed, along the horizontal boundary the dispersion transitions smoothly from having a single minimum at the Γ point to having four minima along the $\Gamma - M$ direction in the Brillouin zone, i.e., the minima move continuously away from the Γ point (which thus becomes a maximum). On the other hand, along the vertical boundary, the minima jump discontinuously from the Γ point to the new four minima, as four local minima at finite momenta dip down to become the global minima. Depending on the value of the chemical potential, there is a region in the T_2/T_1 *vs.* T_3/T_1 plane near the vertical boundary where the Fermi surface has five sheets, four pockets coexisting with a surface surrounding the Γ point. The latter favors s-wave superconductivity as it has no nodes at the Γ point, and it is therefore expected to shift the position of the boundary between d-wave and s-wave superconductivity, as observed.

V. CONCLUSIONS

We presented a slave particle formulation of a mixed boson+fermion quantum dimer model recently proposed in the context of high-T_c superconductors [10–12]. A key finding of this work is that substantial progress can be made using a mean-field analysis that simply assumes a translational and rotational invariant (liquid) state for the bosonic component. We analyze the effective theory

for the remaining fermionic degrees of freedom, and distinguish between two regimes of Fermi surface topology, depending on the effective couplings obtained from both microscopic parameters and correlations of the bosonic liquid state. The two regimes correspond to one Fermi surface around the Γ point, or four Fermi pockets centered along the $\Gamma - M$ lines. By including additional interactions that arise from the $t-J$ model, we find that the system is unstable to superconductivity. The symmetry of the superconducting order parameter, s-wave *vs.* d-wave, is shown to correlate strongly with the Fermi surface topology, with d-wave being favored when four Fermi pockets are present.

Acknowledgements: This work was supported in part by Engineering and Physical Sciences Research Council (EPSRC) Grants No. EP/G049394/1 (C.Ca.) and No. EP/M007065/1 (C.Ca. and G.G.), by DOE Grant DEF-06ER46316 (C.Ch.), and by the EPSRC Network Plus on "Emergence and Physics far from Equilibrium". Statement of compliance with the EPSRC policy framework on research data: this publication reports theoretical work that does not require supporting research data. C.Ca. and G.G. thank the BU visitor program for its hospitality.

[1] D. S. Rokhsar and S. A. Kivelson, Phys. Rev. Lett. **61**, 2376 (1988).

[2] A. Sen, K. Damle and T. Senthil Phys. Rev. B **76**, 235107 (2007); D. Poilblanc, K. Penc, and N. Shannon Phys. Rev. B **75** 220503 (2007); D. Poilblanc, Phys. Rev. B. **76**, 115104 (2007).

[3] A. F. Albuquerque, H. G. Katzgraber, M. Troyer and G. Blatter Phys. Rev. B **78**, 014503 (2008).

[4] R. Moessner and S. L. Sondhi, Phys. Rev. B **68**, 054405 (2003).

[5] R. Moessner, S. L. Sondhi and E. Fradkin, Phys. Rev. B **65**, 024504 (2002).

[6] F. Vernay, A. Ralko, F. Becca and F. Mila, Phys. Rev. B **74**, 054402 (2006).

[7] H. P. Buchler, M. Hermele, S. D. Huber, M. P. A. Fisher and P. Zoller, Phys. Rev. Lett. **95**, 040402 (2005).

[8] E. Fradkin, D. A. Huse, R. Moessner, V. Ognasian and S. L. Sondhi, Phys. Rev. B **69**, 224415 (2004); A. Vishwanath, L. Balents and T. Senthil, Phys. Rev. B **69**, 224415 (2004).

[9] X. G. Wen, *Quantum field theory of many-body systems*, (Oxford University press, Oxford 2004).

[10] M. Punk, A. Allais and S. Sachdev, PNAS **112**, 9552 (2015).

[11] D. Chowdhury and S. Sachdev *The enigma of the pseudogap phase in the cuprate superconductors* in *Quantum criticality in condensed matter: phenomena, materials and ideas in theory and experiment* J. Jedrzejewski eds. (Word scientific publishing co, Singapore 2016).

[12] A. A. Patel, D. Chowdhury, A. Allais, and S. Sachdev, arXiv 1602.05954.

[13] Y. Ando, Y. Kurita, S. Komiya, S. Ono, and K. Segawa, Phys. Rev. Lett. **92**, 197001 (2004).

[14] J. Orenstein, G. A. Thomas, A. J. Millis, S. L. Cooper, D. H. Rapkine, T. Timusk, L. F. Schneemeyer, and J. V. Waszczak, Phys. Rev. B **42**, 6342 (1990).

[15] S. Uchida, T. Ido, H. Takagi, T. Arima, Y. Tokura, and S. Tajima, Phys. Rev. B **43**, 7942 (1991).

[16] P. A. Lee, N. Nagaosa and X. G. Wen, Rev. Mod. Phys. **78** (2006).

[17] A. Damascelli, Z. Hussain, and Z.-X. Shen, Rev. Mod. Phys. 75, 473 (2003).

[18] K. M. Shen, F. Ronning, D. H. Lu, F. Baumberger, N. J. C. Ingle, W. S. Lee, W. Meevasana, Y. Kohsaka, M. Azuma, M. Takano, H. Takagi, and Z.-X. Shen, Science **307**, 901 (2005).

[19] H.-B. Yang, J. D. Rameau, Z.-H. Pan, G. D. Gu, P. D. Johnson, H. Claus, D. G. Hinks, and T. E. Kidd, Phys. Rev. Lett. **107**, 047003 (2011).

[20] J. Gonsalez, M. A. Martin-Delgado, G. Sierra, A. H. Vozmediano, *Quantum electron liquids and high-Tc superconductivity* (Springer, Berlin 1995).

[21] J. Klamut, B. W. Veal, B. M. Dabrowski, P. W. Klamut, M. Kazimerski eds. *Recent developments in high temperature superconductivity* (Springer Verlag, Berlin 1995).

[22] At first glance it appears that there are more gauge transformations that preserve the Hamiltonian. In particular it looks like the transformation $b_{i,\eta} \to e^{i\theta_{i,\eta}} b_{i,\eta}$ and $c_{i,\eta,\sigma} \to e^{i\theta_{i,\eta}} c_{i,\eta,\sigma}$, subject to the constraint that the phases around a plaquette add up to a multiple of 2π $\theta_{i,\hat{x}} - \theta_{i+\hat{x},\hat{y}} + \theta_{i+\hat{y},\hat{x}} - \theta_{i,\hat{y}} = 2\pi n$, is another set of gauge transformations. Here n is an integer and $i, \hat{x}$, $i+\hat{x}, \hat{y}$, $i+\hat{y}, \hat{x}$ and $i, \hat{y}$ are four links arranged counter clockwise around a plaquette. However one can verify (by explicitly constructing the gauge transformations) that every gauge transformation of this form can be written as a gauge transformation of the form in Eq. (3).

[23] See supplementary online information.

[24] M. Ogata, and H. Fukuyama, Rep. Prog. Phys. **71**, 036501 (2008).

[25] K. S. Raman, R. Moessner and S. L. Sondhi, Phys. Rev. B **72**, 064413 (2005).